Available online at www.sciencedirect.com
ScienceDirect
Composite Structures 81 (2007) 374–385
COMPOSITE STRUCTURES
www.elsevier.com/locate/compstruct

Buckling optimization of laminated cylindrical panels subjected to axial compressive load

Hsuan-Teh Hu *, Jiing-Sen Yang

Department of Civil Engineering and Sustainable Environment Research Center, National Cheng Kung University, 1 University Road, Tainan 701, Taiwan, ROC

Available online 6 October 2006

Abstract

The buckling resistance of fiber-reinforced laminated cylindrical panels with a given material system and subjected to uniaxial compressive force is maximized with respect to fiber orientations by using a sequential linear programming method together with a simple move-limit strategy. The significant influences of panel thicknesses, curvatures, aspect ratios, cutouts and end conditions on the optimal fiber orientations and the associated optimal buckling loads of laminated cylindrical panels have been shown through this investigation.

Keywords: Buckling; Optimization; Laminated cylindrical panels; Finite element analysis

1. Introduction

The use of fiber-reinforced laminated cylindrical panels in aerospace and mechanical industries has increased rapidly in recent years. The composite cylindrical panels in service are commonly subjected to various kinds of compressive loads which may cause buckling. Hence, structural instability becomes a major concern in safe and reliable design of the composite cylindrical panels. The buckling resistance of laminated cylindrical panels depends on end conditions, lamination parameters such as ply orientations [1–6], and geometric variables such as thicknesses, curvatures, aspect ratios and cutouts [3,5–10]. Therefore, for composite cylindrical panels with a given material system, geometric shape and end condition, the proper selection of appropriate lamination to realize the maximum buckling resistance of the cylindrical panels becomes a crucial problem.

Research on the subject of structural optimization has been reported by many investigators [11]. Among various optimization schemes, the method of sequential linear programming has been successfully applied to many large scale structural problems [12,13]. Hence, linearization of nonlinear optimization problems to meet requirements for iterative applications of a linear programming method is one of the most popular approaches to solve the structural optimization problem.

In this investigation, buckling optimization of symmetrically laminated cylindrical panels with respect to fiber orientations is performed by using a sequential linear programming method together with a simple move-limit strategy. The critical buckling loads of composite cylindrical panels are calculated by the bifurcation buckling analysis implemented in the ABAQUS finite element program [14]. In this paper, the bifurcation buckling analysis, the constitutive equations for fiber-composite laminate and the optimization method are briefly reviewed first. Then the influence of end conditions, curvatures, aspect ratios, thicknesses and cutouts on the optimal fiber orientations and the associated optimal buckling loads of composite cylindrical panel is presented. Finally, important conclusions obtained from this study are given.

2. Bifurcation buckling analysis

In the finite-element analysis, a system of nonlinear algebraic equations results in the incremental form:

* Corresponding author. Tel.: +886 6 2757575x63168; fax: +886 6 2358542.
E-mail address: hthu@mail.ncku.edu.tw (H.-T. Hu).

0263-8223/$ - see front matter © 2006 Elsevier Ltd. All rights reserved.
doi:10.1016/j.compstruct.2006.08.025

$$[K_t]d\{u\} = d\{p\}, \tag{1}$$

where $[K_t]$ is the tangent stiffness matrix, $d\{u\}$ the incremental nodal displacement vector and $d\{p\}$ the incremental nodal force vector.

Within the range of elastic behavior, it is known that when the deformation of a structure is small, the nonlinear theory leads to the same critical load as the linear theory [15,16]. Consequently, if only the buckling load is to be determined, the calculation can be greatly simplified by assuming the deformation to be small and we can neglect the nonlinear terms which are functions of nodal displacements in the tangent stiffness matrix. The linearized formulation then gives rise to a tangent stiffness matrix in the following expression [17]:

$$[K_t] = [K_L] + [K_\sigma], \tag{2}$$

where $[K_L]$ is a linear stiffness matrix and $[K_\sigma]$ a stress stiffness matrix. If a stress stiffness matrix $[K_\sigma]_{ref}$ is generated according to a reference load $\{p\}_{ref}$, for another load level $\{p\}$ with λ a scalar multiplier, we have

$$\{p\} = \lambda\{p\}_{ref}, \quad [K_\sigma] = \lambda[K_\sigma]_{ref}. \tag{3}$$

When buckling occurs, the external loads do not change, i.e., $d\{p\} = 0$. Then the bifurcation solution for the linearized buckling problem may be determined from the following eigenvalue equation:

$$([K_L] + \lambda_{cr}[K_\sigma]_{ref})d\{u\} = \{0\}, \tag{4}$$

where λ_{cr} is an eigenvalue and $d\{u\}$ becomes the eigenvector defining the buckling mode. The critical load $\{p\}_{cr}$ can be obtained from $\{p\}_{cr} = \lambda_{cr}\{p\}_{ref}$. In ABAQUS, a subspace iteration procedure [18] is used to solve for the eigenvalues and eigenvectors.

3. Constitutive matrix for fiber-composite laminae

In finite element analysis, the laminated cylindrical panels are modeled by eight-node isoparametric laminate shell elements with six degrees of freedom per node (three displacements and three rotations). The formulation of the shell allows transverse shear deformation and this shear flexible shell can be used for both thick and thin shell applications [14].

During the analysis, the constitutive matrices of composite materials at element integration points must be calculated before the stiffness matrices are assembled from element level to global level. For fiber-composite laminate materials, each lamina can be considered as an orthotropic layer. The stress–strain relations for a lamina in the material coordinate (1,2,3) (Fig. 1) at an element integration point can be written as

$$\{\sigma'\} = [Q_1']\{\varepsilon'\}, \quad [Q_1'] = \begin{bmatrix} \frac{E_{11}}{1-\nu_{12}\nu_{21}} & \frac{\nu_{12}E_{22}}{1-\nu_{12}\nu_{21}} & 0 \\ \frac{\nu_{21}E_{11}}{1-\nu_{12}\nu_{21}} & \frac{E_{22}}{1-\nu_{12}\nu_{21}} & 0 \\ 0 & 0 & G_{12} \end{bmatrix}, \tag{5}$$

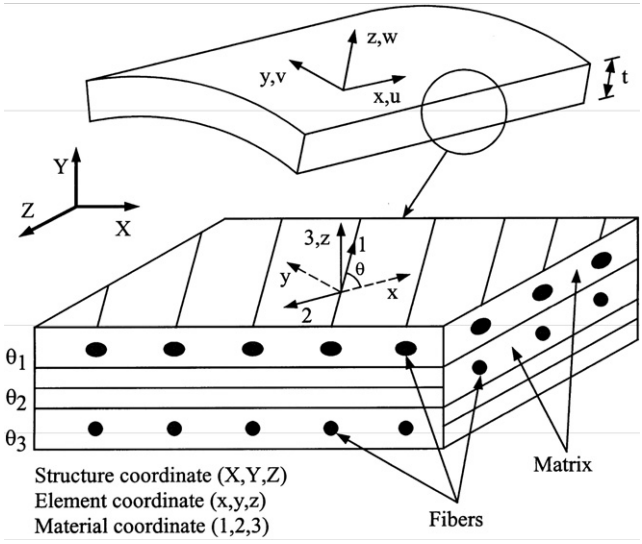

Fig. 1. Material, element and structure coordinates of laminated cylindrical panels.

$$\{\tau'\} = [Q_2']\{\gamma'\}, \quad [Q_2'] = \begin{bmatrix} \alpha_1 G_{13} & 0 \\ 0 & \alpha_2 G_{23} \end{bmatrix}, \tag{6}$$

where $\{\sigma'\} = \{\sigma_1, \sigma_2, \tau_{12}\}^T$, $\{\tau'\} = \{\tau_{13}, \tau_{23}\}^T$, $\{\varepsilon'\} = \{\varepsilon_1, \varepsilon_2, \gamma_{12}\}^T$, $\{\gamma'\} = \{\gamma_{13}, \gamma_{23}\}^T$. It should be noted that the reciprocal relation $\nu_{21}E_{11} = \nu_{12}E_{22}$ is held in Eq. (5). The α_1 and α_2 in Eq. (6) are shear correction factors. In ABAQUS, the shear correction factors are calculated by assuming that the transverse shear energy through the thickness of laminate is equal to that of the case of unidirectional bending [14,19].

The constitutive equations for the lamina in the element coordinate (x, y, z) then become

$$\{\sigma\} = [Q_1]\{\varepsilon\}, \quad [Q_1] = [T_1]^T[Q_1'][T_1], \tag{7}$$

$$\{\tau\} = [Q_2]\{\gamma\}, \quad [Q_2] = [T_2]^T[Q_2'][T_2], \tag{8}$$

$$[T_1] = \begin{bmatrix} \cos^2\theta & \sin^2\theta & \sin\theta\cos\theta \\ \sin^2\theta & \cos^2\theta & -\sin\theta\cos\theta \\ -2\sin\theta\cos\theta & 2\sin\theta\cos\theta & \cos^2\theta - \sin^2\theta \end{bmatrix}, \tag{9}$$

$$[T_2] = \begin{bmatrix} \cos\theta & \sin\theta \\ -\sin\theta & \cos\theta \end{bmatrix}, \tag{10}$$

where $\{\sigma\} = \{\sigma_x, \sigma_y, \tau_{xy}\}^T$, $\{\tau\} = \{\tau_{xz}, \tau_{yz}\}^T$, $\{\varepsilon\} = \{\varepsilon_x, \varepsilon_y, \gamma_{xy}\}^T$, $\{\gamma\} = \{\gamma_{xz}, \gamma_{yz}\}^T$, and fiber orientation θ is measured counterclockwise from the element local x-axis to the material 1-axis.

Let $\{\varepsilon_0\} = \{\varepsilon_{x0}, \varepsilon_{y0}, \gamma_{xy0}\}^T$ be the in-plane strains at the mid-surface of the laminate section, $\{\kappa\} = \{\kappa_x, \kappa_y, \kappa_{xy}\}^T$ the curvatures, and h the total thickness of the section. If there are n layers in the layup, the stress resultants, $\{N\} = \{N_x, N_y, N_{xy}\}^T$, $\{M\} = \{M_x, M_y, M_{xy}\}^T$ and $\{V\} = \{V_x, V_y\}^T$, can be defined as

$$\begin{Bmatrix}\{N\}\\ \{M\}\\ \{V\}\end{Bmatrix}=\int_{-h/2}^{h/2}\begin{Bmatrix}\{\sigma\}\\ z\{\sigma\}\\ \{\tau\}\end{Bmatrix}\mathrm{d}z=\sum_{j=1}^{n}\begin{bmatrix}(z_{j\mathrm{t}}-z_{j\mathrm{b}})[Q_1] & \frac{1}{2}(z_{j\mathrm{t}}^2-z_{j\mathrm{b}}^2)[Q_1] & [0]\\ \frac{1}{2}(z_{j\mathrm{t}}^2-z_{j\mathrm{b}}^2)[Q_1] & \frac{1}{3}(z_{j\mathrm{t}}^3-z_{j\mathrm{b}}^3)[Q_1] & [0]\\ [0]^{\mathrm{T}} & [0]^{\mathrm{T}} & (z_{j\mathrm{t}}-z_{j\mathrm{b}})[Q_2]\end{bmatrix}\begin{Bmatrix}\{\varepsilon_0\}\\ \{\kappa\}\\ \{\gamma\}\end{Bmatrix},\tag{11}$$

where $z_{j\mathrm{t}}$ and $z_{j\mathrm{b}}$ are the distance from the mid-surface of the section to the top and the bottom of the jth layer, respectively. The [0] is a 3 by 2 matrix with all the coefficients equal to zero. It should be noted that in symmetrically laminated composite structures the coupling–stretching stiffness identically vanishes. As a result, the bending and stretching become decoupled in the constitutive equations, i.e.

$$\sum_{j=1}^{n}\frac{1}{2}(z_{j\mathrm{t}}^2-z_{j\mathrm{b}}^2)[Q_1]=\begin{bmatrix}0&0&0\\0&0&0\\0&0&0\end{bmatrix}.\tag{12}$$

4. Sequential linear programming

A general optimization problem may be defined as the following:

$$\text{Minimize}: \quad f(\underline{x}) \tag{13a}$$

$$\text{Subjected to}: \quad g_i(\underline{x})\leqslant 0,\quad i=1,\ldots,r, \tag{13b}$$

$$h_j(\underline{x})=0,\quad j=r+1,\ldots,m, \tag{13c}$$

$$p_k\leqslant x_k\leqslant q_k,\quad k=1,\ldots,n, \tag{13d}$$

where $\underline{x}=\{x_1,x_2,\ldots,x_n\}^{\mathrm{T}}$ is a vector of design variables, $f(\underline{x})$ is an objective function, $g_i(\underline{x})$ are inequality constraints, and $h_j(\underline{x})$ are equality constraints. The p_k and q_k are lower and upper limits of the variable x_k. If an optimization problem requires maximization, we simply minimize $-f(\underline{x})$.

For the optimization problem of Eqs. (13a)–(13d), a linearized problem may be constructed by approximating the nonlinear functions at a current solution point, $\underline{x}_0=\{x_{01},x_{02},\ldots,x_{0n}\}^{\mathrm{T}}$, in a first-order Taylor series expansion as follows:

$$\text{Minimize}: \quad f(\underline{x})\approx f(\underline{x}_0)+\nabla f(\underline{x}_0)^{\mathrm{T}}\delta\underline{x} \tag{14a}$$

$$\text{Subjected to}: \quad g_i(\underline{x})\approx g_i(\underline{x}_0)+\nabla g_i(\underline{x}_0)^{\mathrm{T}}\delta\underline{x}\leqslant 0,\quad i=1,\ldots,r, \tag{14b}$$

$$h_j(\underline{x})\approx h_j(\underline{x}_0)+\nabla h_j(\underline{x}_0)^{\mathrm{T}}\delta\underline{x}=0,\quad j=r+1,\ldots,m, \tag{14c}$$

$$p_k\leqslant x_k\leqslant q_k,\quad k=1,\ldots,n, \tag{14d}$$

where $\delta\underline{x}=\{x_1-x_{01},x_2-x_{02},\ldots,x_n-x_{0n}\}^{\mathrm{T}}$. It is clear that Eqs. (14a)–(14d) represent a linear programming problem where variables are contained in the vector $\delta\underline{x}$. A solution for Eqs. (14a)–(14d) may be easily obtained by the simplex method [20]. After obtaining a solution of Eqs. (14a)–(14d), say $\underline{x}_1$, we can linearize the original problem, Eqs. (13a)–(13d), at $\underline{x}_1$ and solve the new linear programming problem. The process is repeated until a precise solution is achieved. This approach is referred to as sequential linear programming [12,13].

Although the procedure for a sequential linear programming is simple, difficulties may arise during the iterations. First, the optimum solution for the approximate linear problem may violate the constraint conditions of the original optimization problem. Second, in a nonlinear problem, the true optimum solution may appear between two constraint intersections. A straightforward successive linearization may lead to an oscillation of the solution between the widely separated values. Difficulties in dealing with such a problem may be avoided by imposing a "move limit" on the linear approximation [12,13]. The concept of a move limit is that a set of box-like admissible constraints are placed in the range of $\delta\underline{x}$ and it should gradually approach zero as the iterative process continues. It is known that computational economy and accuracy of the approximate solution may depend greatly on the choice of the move limit. In general, the choice of a suitable move

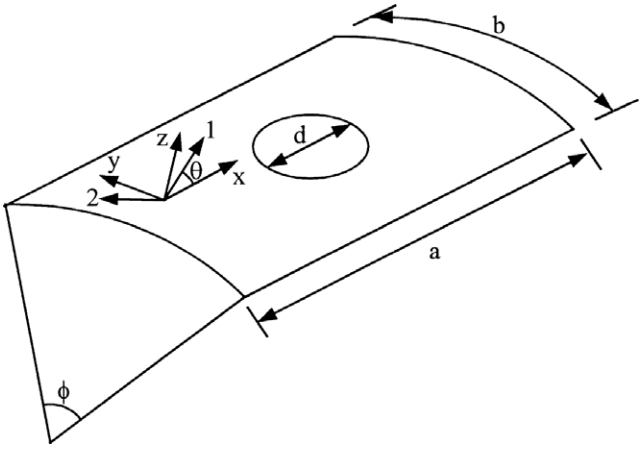

Fig. 2. Laminated cylindrical panel with central circular cutout.

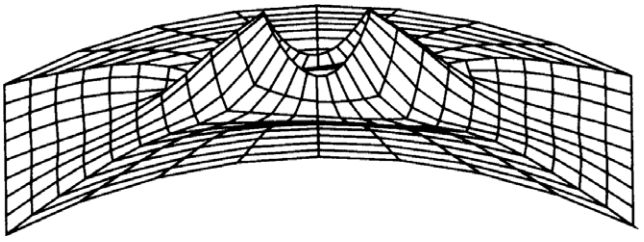

Fig. 3. Critical buckling mode of laminated cylindrical panel with central circular cutout.

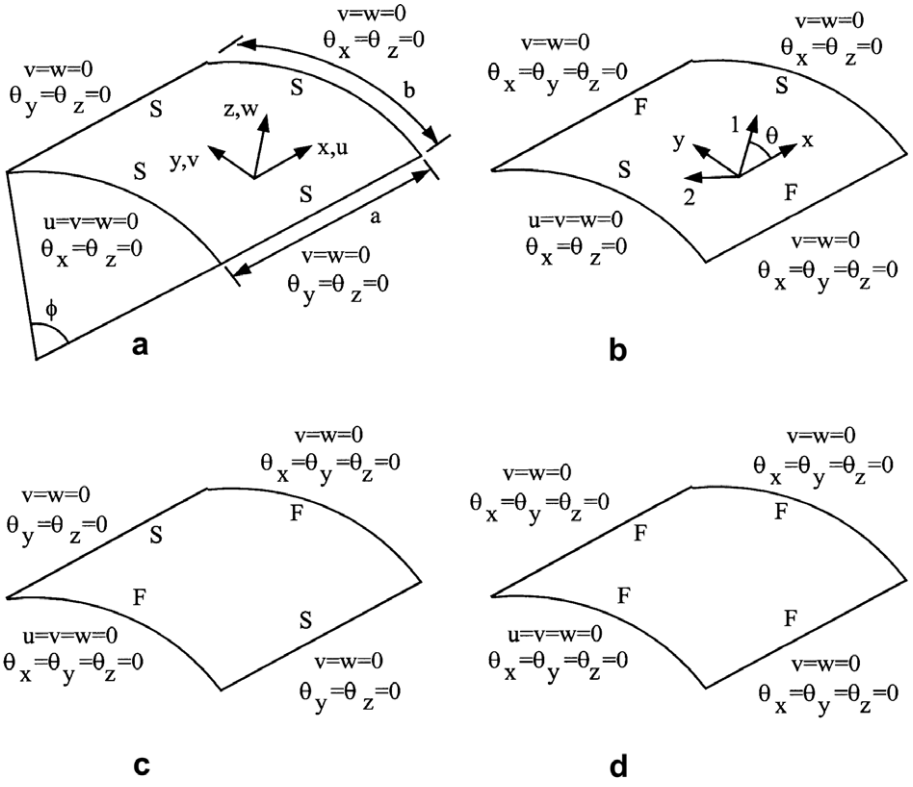

Fig. 4. Laminated cylindrical panels with various end conditions: (a) SSSS panel; (b) SFSF panel; (c) FSFS panel; (d) FFFF panel.

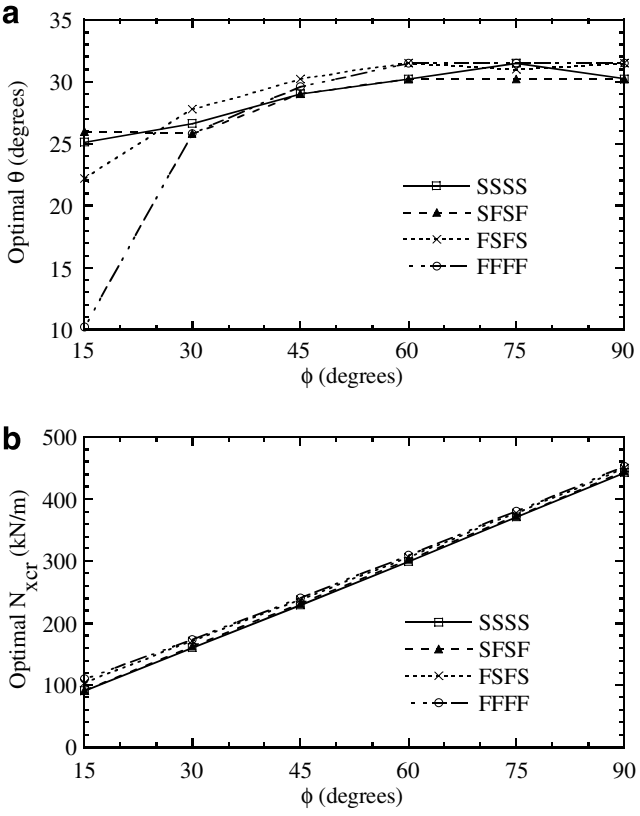

Fig. 5. Effect of end conditions and curvatures on optimal fiber angle and optimal buckling load of thin ($[\pm\theta/90/0]_s$) laminated cylindrical panels ($a/b = 1$): (a) circular angle ϕ vs. optimal fiber angle θ; (b) circular angle ϕ vs. optimal buckling load N_{xcr}.

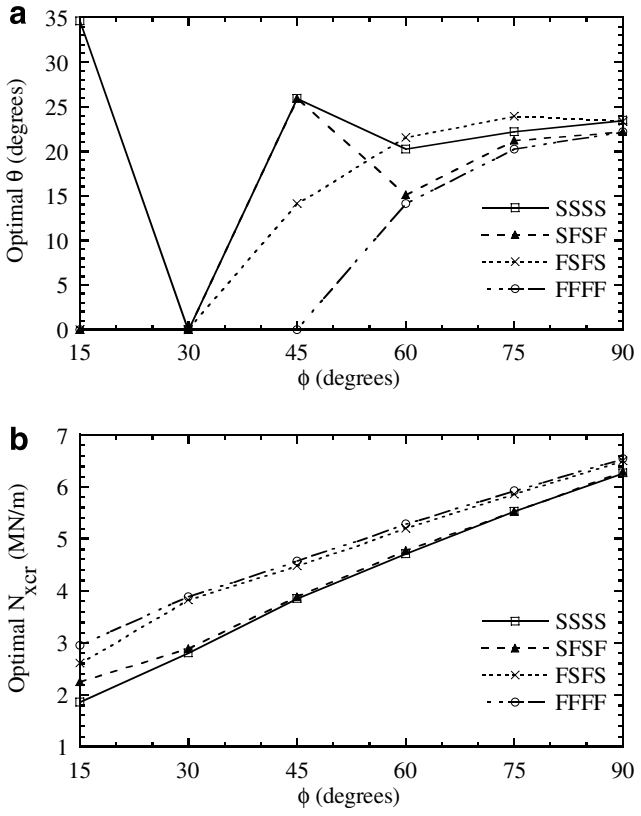

Fig. 6. Effect of end conditions and curvatures on optimal fiber angle and optimal buckling load of thick ($[\pm\theta/90/0]_{4s}$) laminated cylindrical panels ($a/b = 1$): (a) circular angle ϕ vs. optimal fiber angle θ; (b) circular angle ϕ vs. optimal buckling load N_{xcr}.

limit depends on experience and also on the results of previous steps.

The algorithm of the sequential linear programming with selected move limits may be summarized as follows:

(1) Linearize the nonlinear objective function and associated constraints with respect to an initial guess $\underline{x}_0$.
(2) Impose move limits in the form of $-\underline{S} \leqslant (\underline{x} - \underline{x}_0) \leqslant \underline{R}$, where $\underline{S}$ and $\underline{R}$ are properly chosen lower and upper bounds.
(3) Solve the approximate linear programming problem to obtain an optimum solution $\underline{x}_1$.
(4) Repeat the procedures from (1) to (3) by redefining $\underline{x}_1$ with $\underline{x}_0$ until either the subsequent solutions do not change significantly (i.e., true convergence) or the move limit approaches zero (i.e., forced convergence). If the solution obtained is due to forced convergence, the procedures from (1) to (4) should be repeated with another initial guess.

5. Comparison with existing study

The accuracy of the ABAQUS program to predict the buckling load of laminated cylindrical panel is examined in this section by comparing with the experiment data of Knight and Starnes [21] and with the numerical result of Stanley [22]. The dimensions of the tested laminated cylindrical panel are given in Fig. 2. The length of the straight edge a is equal to 35.56 cm, the length of the curved edge b is equal to 36.99 cm and the circular angle ϕ is equal to 55.63°. The panel contains a central circular cutout with diameter d being equal to 5.08 cm. The x, y, z are the axial direction, the hoop direction, and the normal direction of the panels, respectively. The laminated cylindrical panels are subjected to the axial compressive force applied at the curved edges normal to the x direction. The laminate layup of the panel is $[\pm 45/90/0_2/90/\mp 45]_2$ and the thickness of each ply is 0.142 mm. The material constitutive properties as defined by Stanley [22] are $E_{11} = 135$ GPa, $E_{22} = 13$

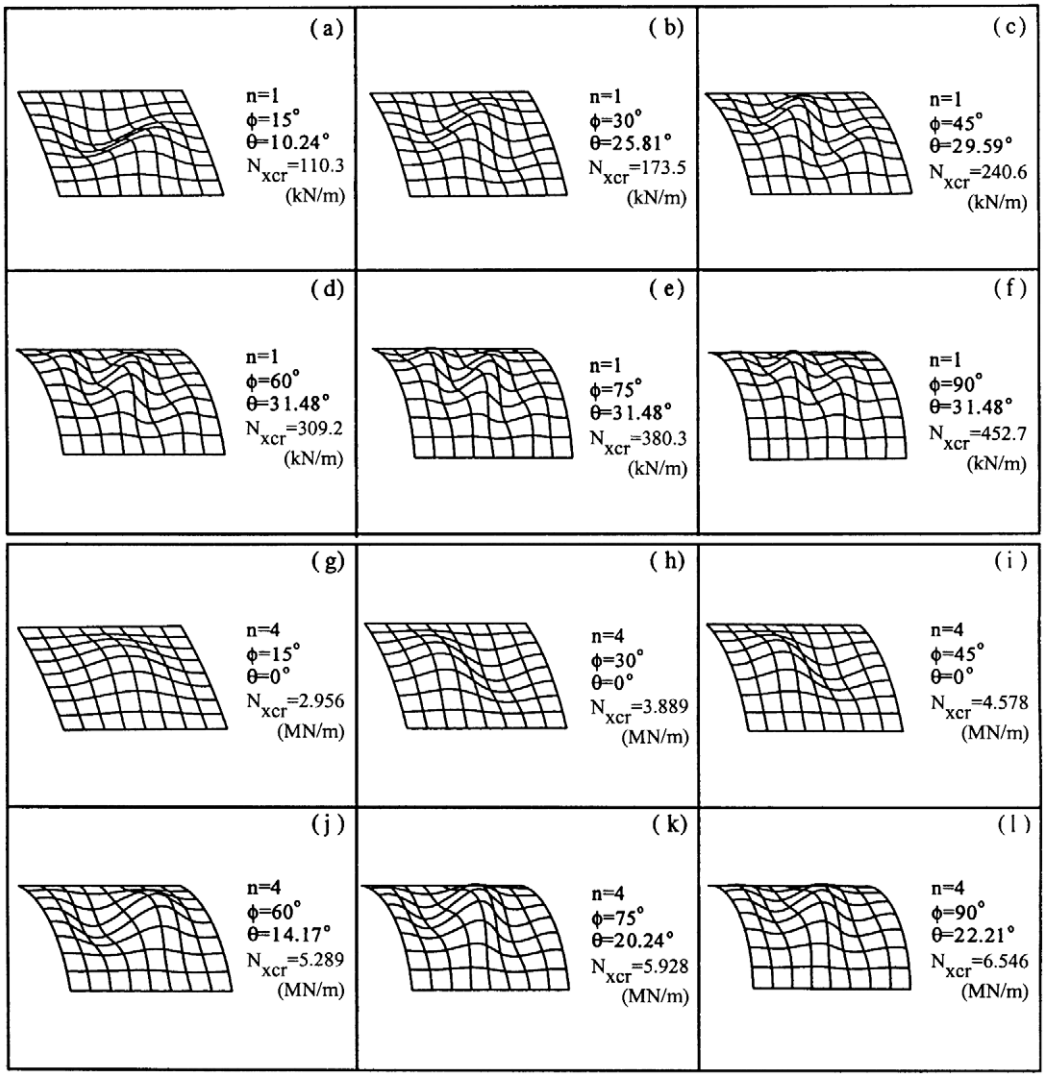

Fig. 7. Typical buckling modes of FFFF laminated cylindrical panels with $[\pm\theta/90/0]_{ns}$ layup and under optimal fiber angles ($a/b = 1$).

GPa, $v_{12} = 0.38$, $G_{12} = G_{13} = 6.4$ GPa, $G_{23} = 4.3$ GPa. The panel is fixed on the left curved edge, fixed except for axial motion on the right curved edge, and simply supported along the two straight edges.

The critical buckling load of the laminated cylindrical panel obtained from the experimental data of Knight and Starnes [21] is 118.7 kN. The critical buckling load of the panel calculated by ABAQUS program and Stanley [22] are 112.9 kN (with 4.9% error) and 107.0 kN (with 9.9% error), respectively. The critical buckling mode obtained by ABAQUS is shown in Fig. 3, which agrees well with that reported by Stanely [22]. As the result, the composite shell elements in ABAQUS program are proved to be able to predict the critical buckling load of laminated cylindrical panel with reasonable accuracy.

6. Results of the optimization analysis

6.1. Laminated cylindrical panels with various curvatures and end conditions

In this section composite laminated cylindrical panels with four types of end conditions (Fig. 4) are considered, which are four edges simply supported (denoted by SSSS), two curved edges simply supported and two straight edges fixed (denoted by SFSF), two curved edges fixed and two straight edges simply supported (denoted by FSFS), and four edges fixed (denoted by FFFF). The laminated cylindrical panels are subjected to the axial compressive load N_x (force per unit length) applied at the edges normal to the x direction. The lengths of the straight edge, a, and the curved edge, b, are both equal to 10 cm and the circular angle ϕ varies between 15° and 90°. The laminate layups of the panels are $[\pm\theta/90/0]_{ns}$ and the thickness of each ply is 0.125 mm. In order to study the influence of panel thickness on the results of optimization, $n = 1$ (8-plies thin panel) and 4 (32-plies thick panel) are selected for analysis. The lamina is consisted of graphite/epoxy (Hercules AS/3501-6) and material constitutive properties are taken from Crawley [23], which are $E_{11} = 128$ GPa, $E_{22} = 11$ GPa, $v_{12} = 0.25$, $G_{12} = G_{13} = 4.48$ GPa, $G_{23} = 1.53$ GPa.

In the finite element analysis, no symmetry simplifications are made for those panels. The boundary conditions (Fig. 4) allow axial displacements u to take place in x direction. Prior to the optimization study, convergence study of the finite element mesh has been performed for $[\pm45/90/0]_s$ and $[\pm45/90/0]_{4s}$ laminated cylindrical panels with $\phi = 60°$ and with all four types of end conditions [24]. On the basis of this study and previous experience [5], it is decided to use 64 elements (8×8 mesh) to model the panels having equal

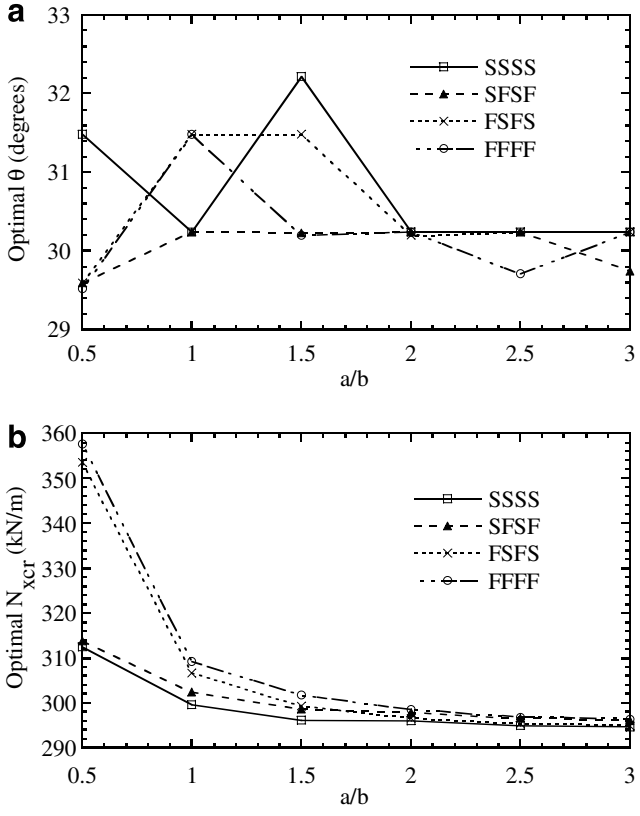

Fig. 8. Effect of end conditions and aspect ratios on optimal fiber angle and optimal buckling load of thin ($[\pm\theta/90/0]_s$) laminated cylindrical panels ($\phi = 60°$): (a) aspect ratio a/b vs. optimal fiber angle θ; (b) aspect ratio a/b vs. optimal buckling load N_{xcr}.

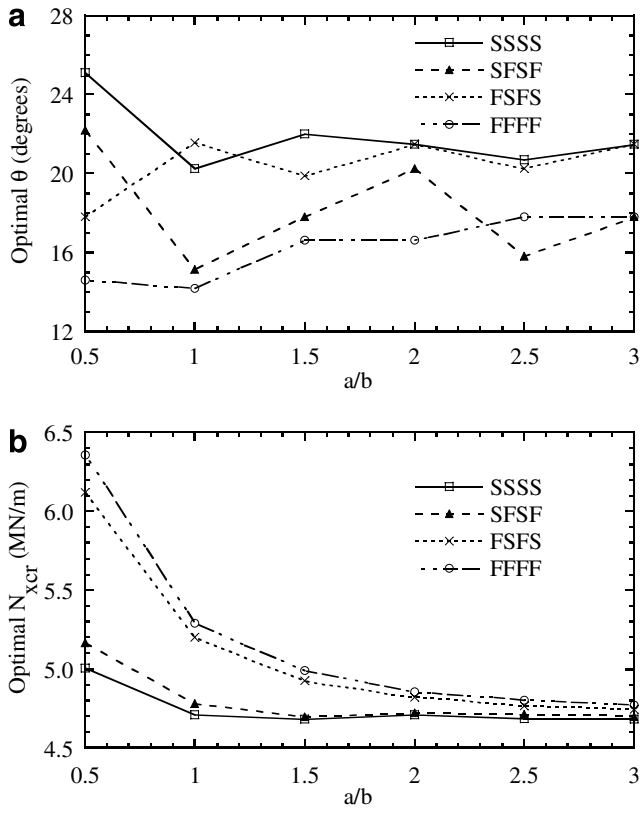

Fig. 9. Effect of end conditions and aspect ratios on optimal fiber angle and optimal buckling load of thick ($[\pm\theta/90/0]_{4s}$) laminated cylindrical panels ($\phi = 60°$): (a) aspect ratio a/b vs. optimal fiber angle θ; (b) aspect ratio a/b vs. optimal buckling load N_{xcr}.

lengths in straight and curved edges. For panels with large aspect ratios or with cutouts, more elements are employed to model the entire structures.

Based on the sequential linear programming method, in each iteration the current linearized optimization problem becomes:

$$\text{Maximize}: \quad N_{xcr}(\theta) \approx N_{xcr}(\theta_0) + (\theta - \theta_0)\left.\frac{\partial N_{xcr}}{\partial \theta}\right|_{\theta=\theta_0} \tag{15a}$$

$$\text{Subjected to}: \quad 0^\circ \leqslant \theta \leqslant 90^\circ, \tag{15b}$$

$$-r \times q \times 0.5^s \leqslant (\theta - \theta_0) \leqslant r \times q \times 0.5^s, \tag{15c}$$

where N_{xcr} is the critical buckling load. The θ_0 is a solution obtained in the previous iteration. The r and q in Eq. (15c) are the size and the reduction rate of the move limit. In the present study, the values of r and q are selected to be 20° and $0.9^{(N-1)}$, where N is a current iteration number. In order to control the oscillation of the solution, a parameter 0.5^s is introduced in the move limit, where s is the number of oscillations of the derivative $\partial N_{xcr}/\partial\theta$ that has taken place before the current iteration. The value of s increases by 1 if the sign of $\partial N_{xcr}/\partial\theta$ changes. Whenever oscillation of the solution occurs, the range of the move limit is reduced to half of its current value. This expedites the solution convergent rate very rapidly.

The $\partial N_{xcr}/\partial\theta$ term in Eq. (15a) may be approximated by using a forward finite-difference method with the following form:

$$\frac{\partial N_{xcr}}{\partial \theta} \approx \frac{[N_{xcr}(\theta_0 + \Delta\theta) - N_{xcr}(\theta_0)}{\Delta\theta}. \tag{16}$$

Hence, to determine the value of $\partial N_{xcr}/\partial\theta$ numerically, two bifurcation buckling analyses to compute $N_{xcr}(\theta_0)$ and $N_{xcr}(\theta_0 + \Delta\theta)$ are needed in each iteration. In this study, the value of $\Delta\theta$ is selected to be 1° in most iterations.

This optimization problem involves only one design variable θ. Though, there are other simple techniques, such as polynomial interpolation and golden section method, available for solving problems of one variable, the sequen-

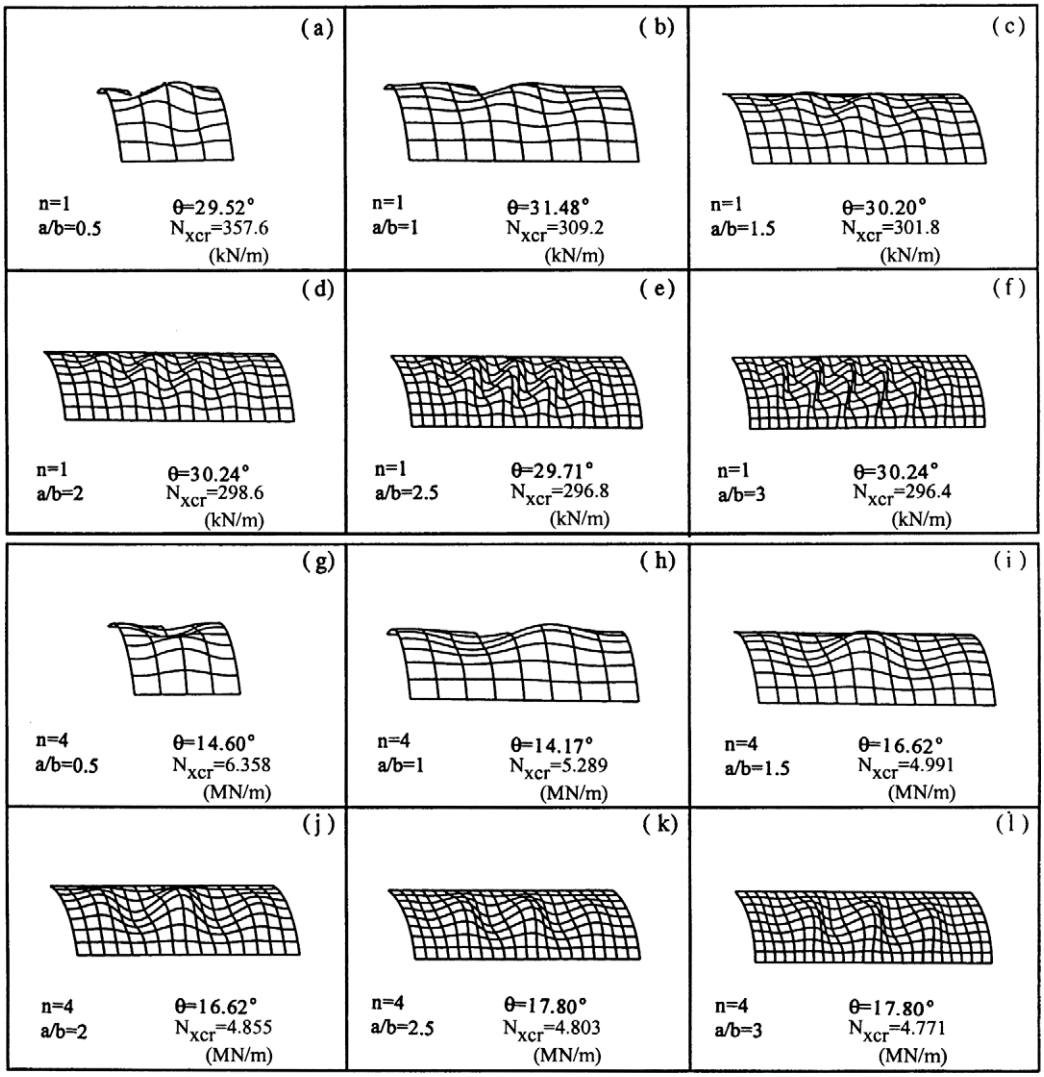

Fig. 10. Typical buckling modes of FFFF laminated cylindrical panels with $[\pm\theta/90/0]_{ns}$ layup and under optimal fiber angles ($\phi = 60°$).

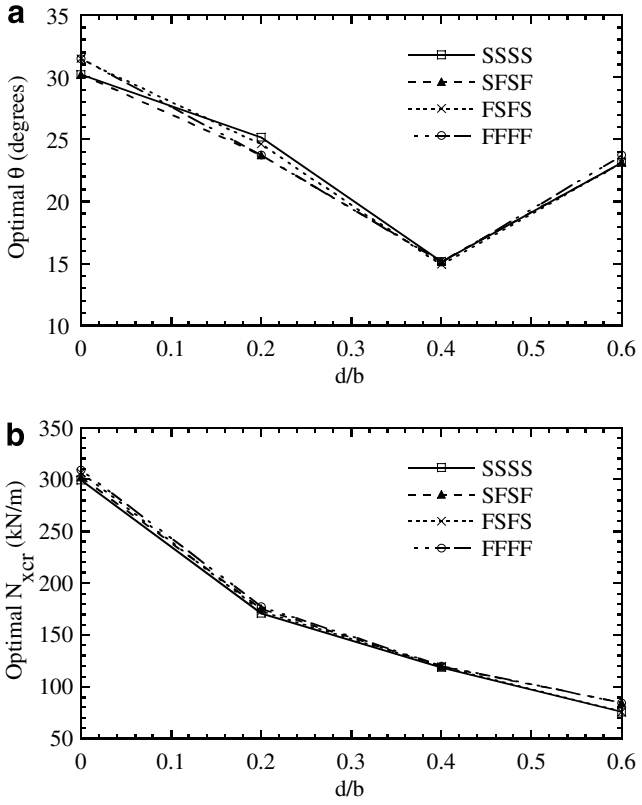

Fig. 11. Effect of end conditions and cutout sizes on optimal fiber angle and optimal buckling load of thin ($[\pm\theta/90/0]_s$) laminated cylindrical panels ($a/b = 1$, $\phi = 60°$): (a) ratio of cutout size d/b vs. optimal fiber angle θ; (b) ratio of cutout size d/b vs. optimal buckling load N_{xcr}.

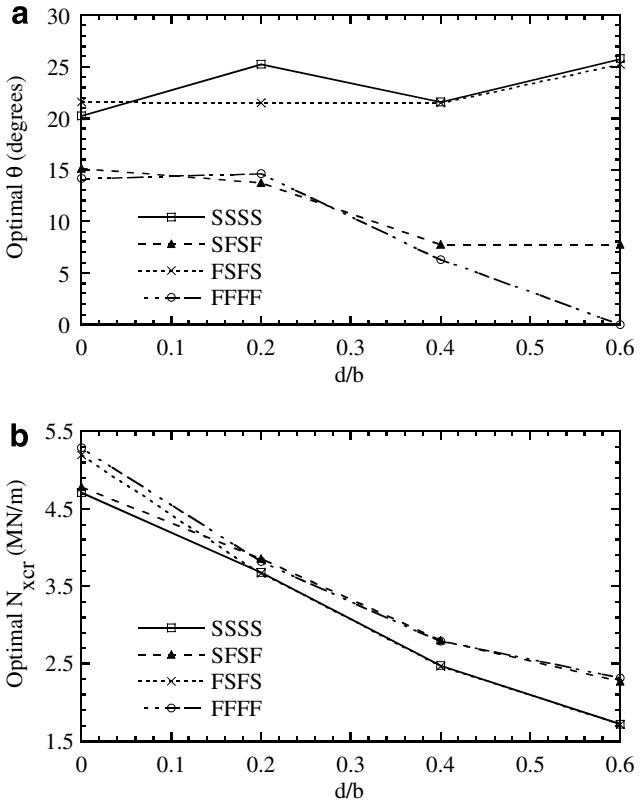

Fig. 12. Effect of end conditions and cutout sizes on optimal fiber angle and optimal buckling load of thick ($[\pm\theta/90/0]_{4s}$) laminated cylindrical panels ($a/b = 1$, $\phi = 60°$): (a) ratio of cutout size d/b vs. optimal fiber angle θ; (b) ratio of cutout size d/b vs. optimal buckling load N_{xcr}.

tial linear programming method is still selected for the optimization. This is because the method can be extended to more variables (i.e., the angles of other plies) easily [13].

Fig. 5 shows the optimal fiber angle θ and the associated optimal buckling load N_{xcr} with respect to the circular angle ϕ for thin ($[\pm\theta/90/0]_s$) laminated cylindrical panels. From Fig. 5a, we can see that when ϕ is less than 30°, the end conditions have significant influence on optimal fiber angles of the panels. However, when ϕ is greater than 30°, the optimal fiber angles of these panels with different end conditions seem to be very close. Fig. 5b shows that the optimal buckling load N_{xcr} increases with the increase of the circular angle ϕ. Among these panels under the same geometric configuration, the FFFF panels have the highest optimal buckling loads, and the SSSS panels have the lowest optimal buckling loads. In addition, the optimal buckling loads of SFSF panels are very close to those of SSSS panels, and the optimal buckling loads of FSFS panels are very similar to those of FFFF panels. This indicates the panels at this geometric configuration are governed by the boundary conditions at the curved edges.

Fig. 6 shows the optimal fiber angle θ and the associated optimal buckling load N_{xcr} with respect to the circular angle ϕ for thick ($[\pm\theta/90/0]_{4s}$) laminated cylindrical panels. Fig. 4a shows that when ϕ is less than 75°, the end conditions have significant influence on optimal fiber angle θ of the panels. Comparing Fig. 6a with Fig. 5a, we can observe that thickness has significant influence on the optimal fiber angles of the cylindrical panels. From Fig. 6b we can observe that the buckling strengths of these thick panels are also governed by the boundary conditions at the curved sides and the optimal buckling load increases with the increase of the panel curvature as thin panels.

Fig. 7 shows the typical buckling modes for both thin and thick ($[\pm\theta/90/0]_s$ and $[\pm\theta/90/0]_{4s}$) panels with four fixed ends and under an optimal fiber orientation. We find that as panel curvatures increase, the buckling modes of these panels have more waves in the axial direction. Similar results are also obtained for panels with other end conditions [24].

6.2. Laminated cylindrical panels with various aspect ratios and end conditions

In this section, laminated cylindrical panels with various aspect ratios a/b are analyzed. The length of the curved edge, b, is equal to 10 cm and the length of the straight edge, a, varies between 5 and 30 cm (Fig. 4). The circular angle, ϕ, of these panels is set to 60°. Four types of end conditions, i.e., SSSS, SFSF, FSFS, and FFFF, described in a previous section are considered. Again, the laminate layups, $[\pm\theta/90/0]_s$ and $[\pm\theta/90/0]_{4s}$, are selected for analysis.

Fig. 8 shows the optimal fiber angle θ and the associated optimal buckling load N_{xcr} with respect to the aspect

ratio a/b for thin ($[\pm\theta/90/0]_s$) laminated cylindrical panels. From Fig. 8a, we can see that the results of optimization for these panels with different end conditions vary between 29° and 32°. The results in Fig. 8b show that as a/b increases, the optimal buckling loads of these panels diminish to constant values. Generally, when the aspect ratio is small (say $a/b < 1$), the results of optimization for SFSF panels are similar to those of SSSS panels and the results of optimization for FSFS panels are similar to those of FFFF panels. However, when the aspect ratio is large (say $a/b > 2$), the results of optimization for SFSF panels are similar to those of FFFF panels and the results of optimization for FSFS panels are similar to those of SSSS panels. This indicates that the panels are governed by the boundary conditions at the curved edges for short panels and governed by the boundary conditions at the straight edges for long panels.

Fig. 9 shows the optimal fiber angle θ and the associated optimal buckling load N_{xcr} with respect to the aspect ratio a/b for thick ($[\pm\theta/90/0]_{4s}$) laminated cylindrical panels. Fig. 9a indicates that the results of optimization for these panels with different end conditions vary between 14° and 25°. Fig. 9b shows a trend similar to Fig. 8b except that the values of the optimal buckling loads of thick panels are higher than those of thin panels. Typical buckling modes for both thin and thick ($[\pm\theta/90/0]_s$ and $[\pm\theta/90/0]_{4s}$) panels with four fixed ends and under optimal fiber orientations are given in Fig. 10. We can find that as the panel aspect ratio increase, the buckling modes of these panels have more waves in the axial direction. Similar results are also obtained for panels with other end conditions [24].

6.3. Laminated cylindrical panels with various central circular cutouts and end conditions

In this section, laminated cylindrical panels with $a = b = 10$ cm, $\phi = 60°$ are analyzed (Fig. 2). These panels

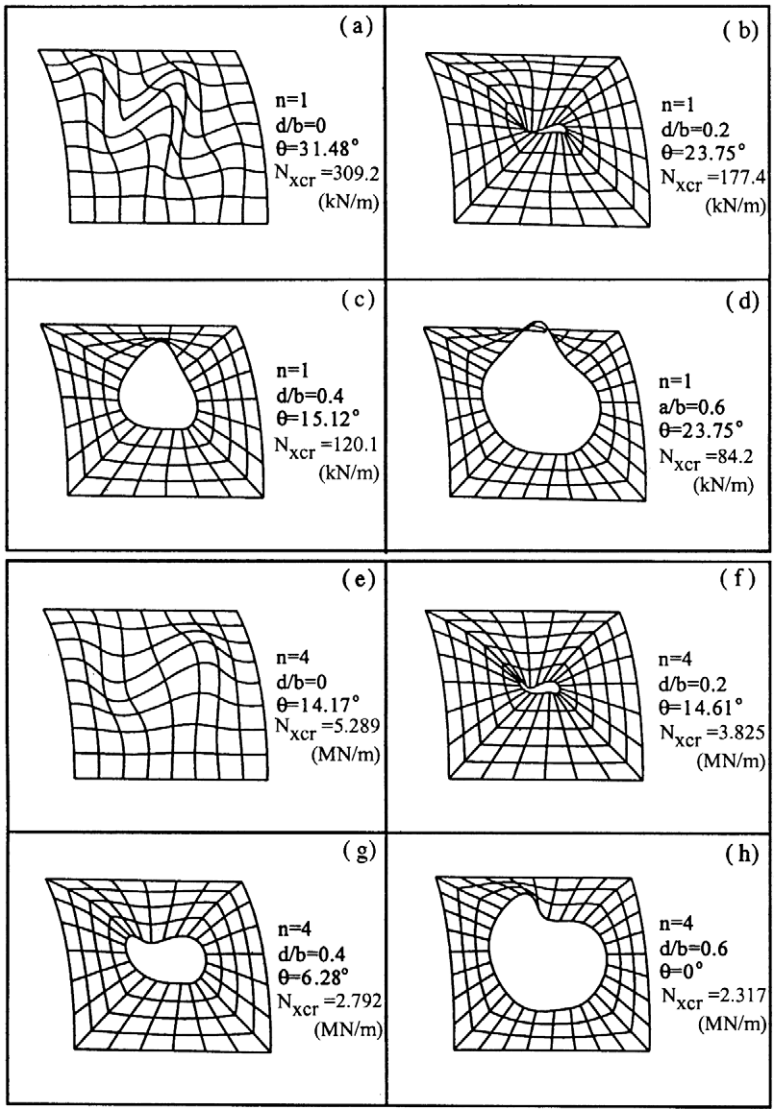

Fig. 13. Typical buckling modes of FFFF laminated cylindrical panels with central circular cutout, with $[\pm\theta/90/0]_{ns}$ layup and under optimal fiber angles ($a/b = 1$, $\phi = 60°$).

contain central circular cutouts with diameter d which varies between 0 and 6 cm. As before, four types of end conditions and two laminate layups, $[\pm\theta/90/0]_s$ and $[\pm\theta/90/0]_{4s}$, are selected for analysis.

Fig. 11 shows the optimal fiber angle θ and the associated optimal buckling load N_{xcr} with respect to the ratio d/b for thin ($[\pm\theta/90/0]_s$) laminated cylindrical panels. From Fig. 11a, we can see that the edge conditions have very little influence on the optimal fiber angle θ and θ seems to be a second order function of the d/b ratio. Fig. 11b shows that the optimal buckling loads decrease with the increase of the cutout sizes, which is not surprised.

Fig. 12 shows the optimal fiber angle θ and the associated optimal buckling load N_{xcr} with respect to the ratio d/b for thick ($[\pm\theta/90/0]_{4s}$) laminated cylindrical panels. Fig. 12a indicates that these thick panels are governed by the boundary conditions at the straight edges and the values of optimal fiber angles of SFSF panels and FFFF panels are smaller than those of FSFS panels and SSSS panels. Fig. 12b again shows that the optimal buckling loads decrease with the increase of the d/b ratio.

Typical buckling modes for both thin and thick ($[\pm\theta/90/0]_s$ and $[\pm\theta/90/0]_{4s}$) panels with four fixed ends and under optimal fiber orientations are given in Fig. 13. These modes show that when the cutout sizes are small, the buckling modes are global (i.e., buckling of entire panel). However, when the cutout sizes are large, the buckling modes are local (i.e., buckling of panel area near hole). Similar results are also obtained for panels with other end conditions [24].

6.4. Laminated cylindrical panels containing central circular cutouts with various aspect ratios and end conditions

In this section, laminated cylindrical panels with $b = 10$ cm, $\phi = 60°$ are analyzed (Fig. 2). The length of the straight edge, a, varies between 10 and 30 cm. These panels contain central circular cutouts with diameter $d = 6$ cm. As before, four types of end conditions, SSSS, SFSF, FSFS, FFFF, and two laminate layups, $[\pm\theta/90/0]_s$ and $[\pm\theta/90/0]_{4s}$, are selected for analysis.

Figs. 14 and 15 show the optimal fiber angle θ and the associated optimal buckling load N_{xcr} with respect to the aspect ratio a/b for both thin and thick ($[\pm\theta/90/0]_s$ and $[\pm\theta/90/0]_{4s}$) laminated cylindrical panels. Figs. 14a and 15a show that, generally, the optimal fiber angles increase with the increase of panel aspect ratio. For $[\pm\theta/90/0]_s$ panels, the optimal fiber angles of SFSF and FFFF conditions are greater than those of FSFS and SSSS conditions. However, for $[\pm\theta/90/0]_{4s}$ panels, the optimal fiber

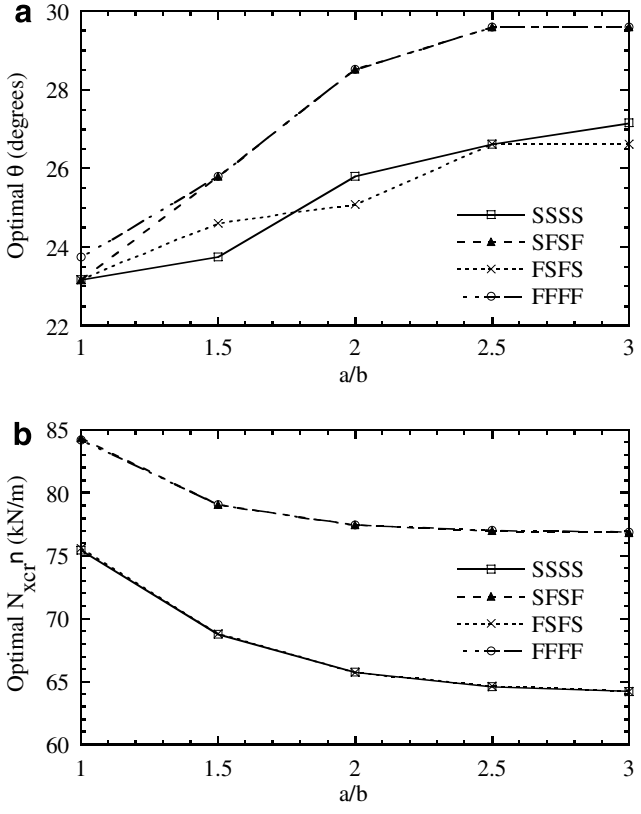

Fig. 14. Effect of end conditions and aspect ratios on optimal fiber angle and optimal buckling load of thin ($[\pm\theta/90/0]_s$) laminated cylindrical panels with central circular cutout ($d/b = 0.6$, $\phi = 60°$): (a) aspect ratio a/b vs. optimal fiber angle θ; (b) aspect ratio a/b vs. optimal buckling load N_{xcr}.

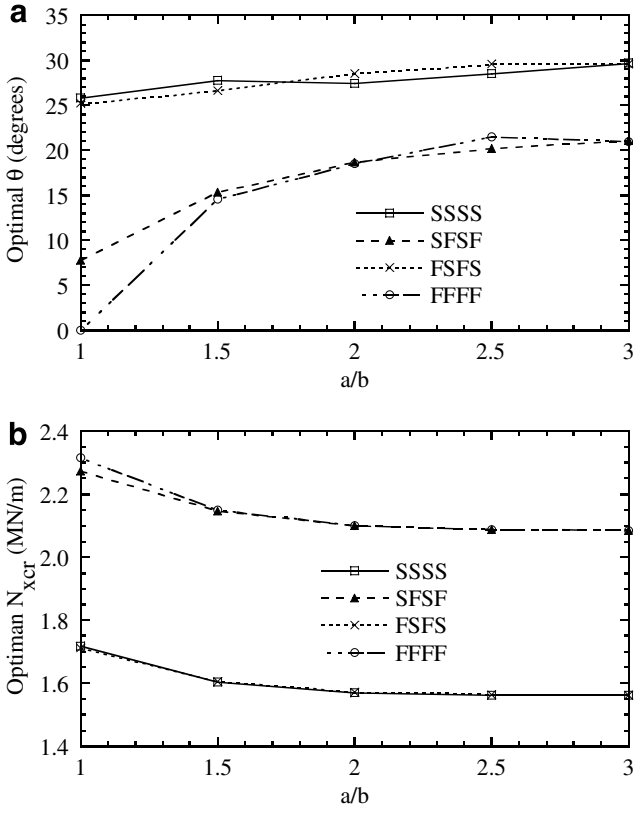

Fig. 15. Effect of end conditions and aspect ratios on optimal fiber angle and optimal buckling load of thick ($[\pm\theta/90/0]_{4s}$) laminated cylindrical panels with central circular cutout ($d/b = 0.6$, $\phi = 60°$): (a) aspect ratio a/b vs. optimal fiber angle θ; (b) aspect ratio a/b vs. optimal buckling load N_{xcr}.

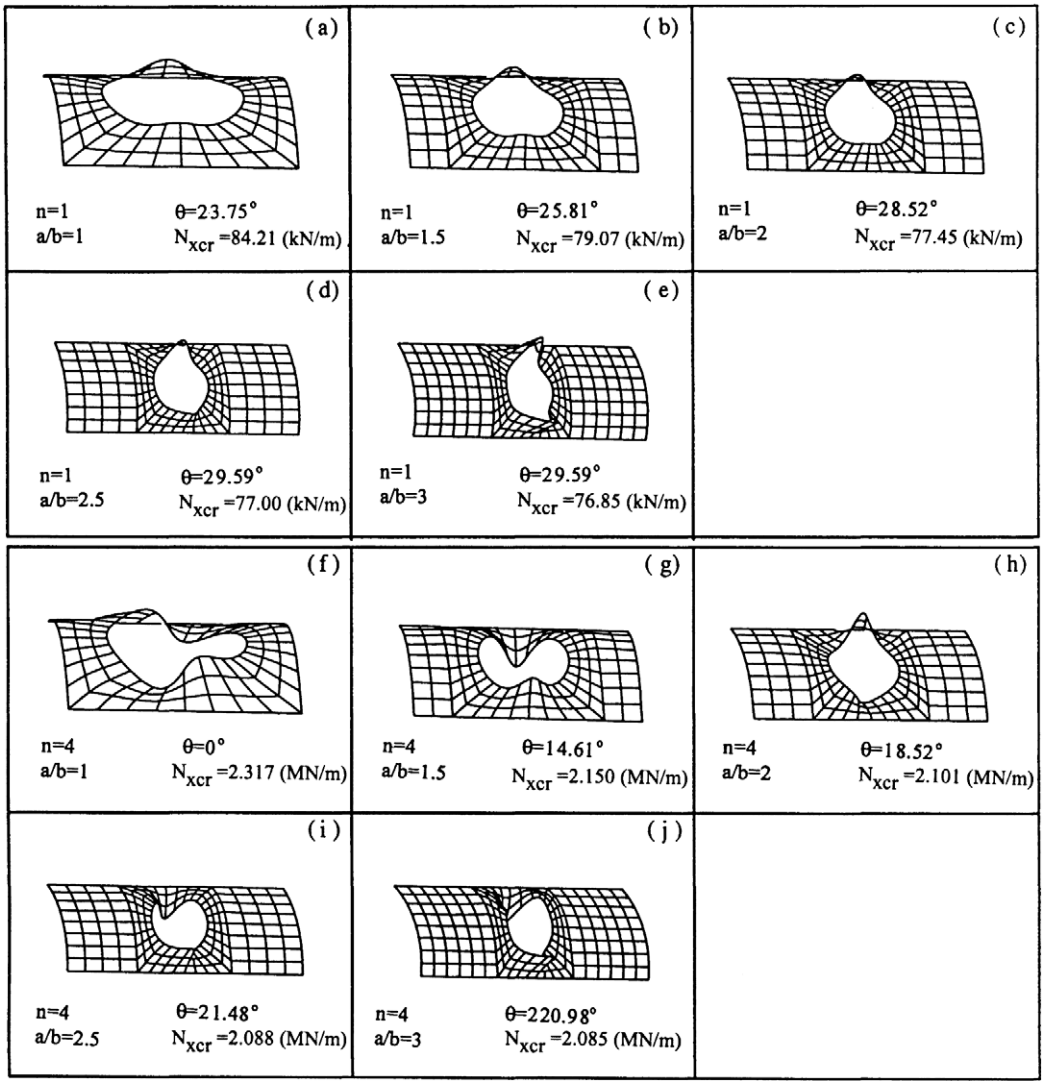

Fig. 16. Typical buckling modes of FFFF laminated cylindrical panels with central circular cutout, with $[\pm\theta/90/0]_{ns}$ layup and under optimal fiber angles ($d/b = 0.6$, $\phi = 60°$).

angles of SFSF and FFFF conditions are smaller than those of FSFS and SSSS conditions. Comparing Figs. 14a and 15a with Figs. 8a and 9a, we can see that the cutouts have significant influence on the optimal fiber angles of curved panels. From Figs. 14b and 15b we can see that as *a*/*b* increases, the optimal buckling loads of these panels gradually decrease and diminish to constant values. In spite of the thickness, the buckling strengths of these panels are governed by the boundary conditions at the straight edges.

Typical buckling modes for both thin and thick ($[\pm\theta/90/0]_s$ and $[\pm\theta/90/0]_{4s}$) panels with four fixed ends and under optimal fiber orientations are given in Fig. 16. These modes show that when the panel aspect ratios are small, the buckling modes are associated to the entire panel. However, when the panel aspect ratios are large, the buckling modes are usually local around the cutout areas. Similar results are also obtained for panels with other end conditions [24].

7. Conclusions

For the optimal buckling analysis of uniaxially compressed symmetrically laminated cylindrical panels with different thicknesses, aspect ratios, circular cutouts and end conditions, the following conclusions may be drawn:

1. Thickness has significant influence on the optimal fiber angles of the cylindrical panels without cutouts. The optimal buckling loads of these cylindrical panels increase with the increasing of panel curvature and are governed by the boundary conditions at the curved sides. In addition, the buckling modes of these panels would have more waves in the axial direction if the panel curvatures are increased.
2. The optimal buckling loads of the panels without cutout are governed by the boundary conditions at the curved edge for short panels and by the boundary conditions at the straight edge for long panels. In addition, the

optimal buckling loads of these cylindrical panels decrease with the increasing of panel aspect ratios. The buckling mode of these panels would have more waves in the axial direction if the panel aspect ratios are increased.

3. The optimal buckling loads of the panels with cutout decrease with the increasing of cutout size. For thin panel, the edge conditions have very little influence on the optimal fiber angle as well as the optimal buckling load. However, the buckling behavior of the thick panel is governed by the boundary conditions at the straight edge. When the cutout sizes are small, the buckling modes are global for the entire panels. However, when the cutout sizes are large, the buckling modes are local around the cutout areas.
4. The optimal buckling loads of the panels with cutout also decrease with the increasing of panel aspect ratios. When the panel aspect ratios are small, the buckling modes are associated to the entire panel. However, when the panel aspect ratios are large, the buckling modes are local around the cutout areas.

References

[1] Crouzet-Pascal J. Buckling analysis of laminated composite plates. Fibre Sci Technol 1978;11:413–46.

[2] Hirano Y. Optimum design of laminated plates under axial compression. AIAA J 1979;17:1017–9.

[3] Leissa AW. Buckling of laminated composite plates and shell panels. AFWAL-TR-85-3069, Flight Dynamics Laboratory, Air Force Wright Aeronautical Laboratories, Wright-Patterson Air Force Base, OH; 1985.

[4] Muc A. Optimal fibre orientation for simply-supported angle-ply plates under biaxial compression. Compos Struct 1988;9:161–72.

[5] Hu HT, Lin BH. Buckling optimization of symmetrically laminated rectangular plates with various geometry and end conditions. Compos Sci Technol 1995;55:277–85.

[6] Turvey GJ, Marshall IH. Buckling and postbuckling of composite plates. London: Chapman & Hall; 1995.

[7] Rhodes MD, Mikulas MM, McGowan PE. Effects of orthotropy and width on the compression strength of graphite-epoxy panels with holes. AIAA J 1984;22:1283–92.

[8] Nemeth MP. Importance of anisotropy on buckling of compression-loaded symmetric composite plates. AIAA J 1986;24:1831–5.

[9] Nemeth MP. Buckling behavior of compression-loaded symmetrically laminated angle-ply plates with holes. AIAA J 1988;26:330–6.

[10] Vellaichamy S, Prakash BG, Brun S. Optimum design of cutouts in laminated composite structures. Comput Struct 1990;37:241–6.

[11] Schmit LA. Structural synthesis – its genesis and development. AIAA J 1981;19:1249–63.

[12] Zienkiewicz OC, Champbell JS. Shape optimization and sequential linear programming. In: Gallagher RH, Zienkiewicz OC, editors. Optimum structural design, theory and applications. New York: Wiley; 1973. p. 109–26.

[13] Vanderplaats GN. Numerical optimization techniques for engineering design with applications. New York: McGraw-Hill; 1984 [Chapter 6].

[14] ABAQUS, Inc., ABAQUS analysis user's manuals and example problems manuals, Version 6.5. Providence, RI; 2005.

[15] Wang CT. Applied elasticity. New York: McGraw-Hill; 1953 [Chapter 9].

[16] Chajes A. Principles of structural stability theory. Englewood Cliffs (NJ): Prentice-Hall; 1974 [Chapter 1].

[17] Cook RD, Malkus DS, Plesha ME. Concepts and applications of finite element analysis. 4th ed. New York: Wiley; 2002 [Chapter 18].

[18] Bathe KJ, Wilson EL. Large eigenvalue problems in dynamic analysis. J Eng Mech Div ASCE 1972;98:1471–85.

[19] Whitney JM. Shear correction factors for orthotropic laminates under static load. J Appl Mech 1973;40:302–4.

[20] Kolman B, Beck RE. Elementary linear programming with applications. Orlando: Academic Press; 1980 [Chapter 2].

[21] Knight NF, Starnes JH. Postbuckling behavior of axially compressed graphite-expoxy cylindrical panels with circular holes. Presented at the 1984 ASME joint pressure vessels and piping/applied mechanics conference, San Antonio, TX; 1984.

[22] Stanley GM. Continuum-based shell elements. PhD Thesis, Department of Mechanical Engineering, Stanford University; 1985.

[23] Crawley EF. The natural modes of graphite/epoxy cantilever plates and shells. J Compos Mater 1979;13:195–205.

[24] Yang, J-S. The effect of geometry and end conditions on the buckling optimization of laminated cylindrical panels subjected to axial compressive forces. MS Thesis, Department of Civil Engineering, National Cheng Kung University, Tainan, Taiwan, ROC; 1999.